



# A systematic study of structural and electronic properties of beryllium and nitrogen co-doped stanene for optoelectronic application


Dauda Abubakar<sup>1</sup>, Abdullahi Lawal<sup>2\*</sup>, Rakiya Haruna<sup>3</sup> and Musa Bello<sup>3</sup>

<sup>1</sup>Department of Physics, Faculty of Science, Sa'adu Zungur University Gadua, Bauchi State, Nigeria.

<sup>2</sup>Department of Physics, Ahmadu Bello University, Zaria, Kaduna State, Nigeria.

<sup>3</sup>Department of Physics, Federal College of Education, Zaria, Kaduna State, Nigeria.

\*Correspondence: [abdullahikubau@yahoo.com](mailto:abdullahikubau@yahoo.com) +2347033860054

Abstract	Article History
<p>This paper investigates the structural and electronic properties of doped/co-doped stanene with Be and N atoms using first principles calculations. The computed lattice parameters, bond length and bond angle with van der Waals corrections (vdW-DFC09x) were found to be close to the experimental results. Band structure calculations revealed that pure stanene is a zero-band gap material with Dirac cone located at K-point and this matched very well with previous theoretical and experimental results. Be doped stanene exhibits a band gap above the Fermi level of 0.29, 0.56 and 1.1 eV for 5.6 %, 11.1 % and 16.7 % concentrations, indicating that Be doped stanene could behave as degenerate semiconductor. For N doped stanene the band-gap below the Fermi level were 0.30, 0.45 and 0.96 eV for 5.6 %, 11.1 % and 16.7 % doping concentrations. Our results show that there is transition from metallic nature as in the case of pure stanene to semiconductor for Be and N mono-doped stanene. Additionally, Be-N co-doped stanine opens up a wider band gap in comparison with the mono doping. A band gap value of 1.24 eV was formed above the Fermi level in the case of Be-N co-doping showing p-type character. Accordingly, our findings suggested that Be-N co-doped stanene is a promising material for optoelectronic, solar and other application like Be-N co-doped graphene.</p>	<p>Received: 11/07/2024 Accepted: 29/11/2024 Published: 31/12/2024</p>
	<p><b>Keywords:</b> DFT, Stanene, Co-doping, Solar cells.</p>
	<p><b>License:</b> CC BY 4.0*</p>  <p><b>Open Access Article</b></p>
<p><b>How to cite this paper:</b> Dauda, A., Abdullahi L., Rakiya, H., and Musa B., (2024) A systematic study of structural and electronic properties of beryllium and nitrogen co-doped stanene for optoelectronic application <i>Gadua J Pure Alli Sci</i>, 3(2): 63-69. <a href="https://doi.org/10.54117/gjpas.v3i2.147">https://doi.org/10.54117/gjpas.v3i2.147</a></p>	

## 1.0 Introduction

Recently, Two-dimensional materials have received a lot of attention because of exceptional characteristics they demonstrated in electronic and optical properties (Baig, 2023; Gidado et al., 2024; Shuaibu *et al.*, 2021). Following the discovery of graphene, heavy group-IV elements (Si, Ge, and Sn) are currently receiving a lot of attention due to their similar electronic properties. Examples include the properties of massless Dirac Fermions in charge carriers formed via linear band dispersion at the Fermi energy.

Recently, several experimental approaches have been used to create 2D materials (Geng & Yang, 2018). Silicene and germanene based honeycomb-like buckled structures have been synthesized using molecular beam epitaxy method (Abbasi & Sardroodi, 2018). Different allotropes of atomically thin tin have been theoretically predicted by Garcia and co-workers (Garcia *et al.*, 2011). They have suggested that tin-based allotropes exhibit properties similar to graphene. Stanene as one of the imperative largest honeycomb-like structure its shows attractive

properties such as Dirac-cone, high carrier mobility and unfortunately with unfavorable zero energy band-gap (Abbasi, 2019). Generally, stanene has numerous applications such as energy storage, energy conversion and photocatalyst. Zero band gap of stanene has been confirmed by numerous first principles calculation without inclusion of spin-orbit coupling (SOC) (Nagarajan & Chandiramouli, 2017; Taura *et al.*, 2021; Zhao *et al.*, 2024). However, inclusion of SOC created a band gap of about 0.1eV, which designates its potentiality for next-generation optoelectronic applications. Furthermore, suitable chemical functionalization produces a band gap of 0.3 eV (Chen *et al.*, 2024; Zhang *et al.*, 2014). Thus, tuning the fundamental band gap of stanene has triggered enormous interest in fabricating and designing electronic devices with high performance (Itas, Suleiman, Ndikilar, Lawal, Razali, Ullah, *et al.*, 2023; Qi *et al.*, 2021). The most important limitation of utilizing pristine stanene for optoelectronic application is its gapless nature. Conversely, Garg *et al.* used Vienna Ab Initio Simulation Package (VASP) to investigate the effects of doping Borron (B)/Nitrogen (N) elements into stanene structure and significant improvements in band gap opening has been achieved around the Fermi level (Garg *et al.*, 2017). However, based on our knowledge there is no detailed studied on Be/N co-doped stanene nanosheets. Thus, doped stanene monolayer could be a promising candidate for a large diversity of applications. Therefore, the potential for a band gap to arise in stanene is of tremendous scientific interest. Diverse methods have been used to alter the electronic properties of pure stanene. For instance, Tang *et al.* recommended that electronic properties of pure stanene can be modify via functionalization (Tang *et al.*, 2021; Xu *et al.*, 2015). Wang and co-workers reported that stanene/hexagonal boron nitride (hBN) heterostructure produces a sizable band gap when compared to pure stanene (Wang *et al.*, 2014). Several studies suggested that doping is one of the efficient methods to modify the band gap of 2D materials (Chaves *et al.*, 2020; Lawal *et al.*, 2021; Nandee *et al.*, 2022; Yang *et al.*, 2024). The structural and electronic properties of Be-N co-doped stanene are examined in this paper by substitutional elemental approach using first-principles calculations within density functional theory (DFT) framework exposed to acute concentrations.

## 2.0 Computational Method

In this work, Quantum Espresso and Yambo codes were used for converging test, electronic and structural properties calculations. For treating exchange-correlation functional, generalized Gradient approximation (GGA) as proposed by Perdew-Burke-Ernzerh of (PBE) was used. We set convergence tolerance to be  $10^{-3}$  and  $10^{-5}$  eV/Å for force and total energy for all self-consistency calculations (Mubashir *et al.*, 2024; Ziesche *et al.*, 1998). In the case of expanding electronic wave functions and charge density, a

Kinetic energy cut offs of 50 Ry and 280 Ry were used for all the calculations. Structurally, stanene has low-buckled honeycomb structure containing two atoms arranged in hexagonal structure and this geometry is the most stable structure (Liu *et al.*, 2022). The stable structure of stanene has weak  $\pi - \pi$  bonding between the tin atoms. Presence of buckling and weak bonding increases the stability in stanene due to increase in overlapping between  $\sigma$  and  $\pi$  and orbitals. The first Brillouin zone (BZ) of the system constructed from the two-atom unit cell is integrated with Monk-horst Pack grid of (12 12 1) for structural and electronic properties calculations. The constructed system considered in this work containing 18 atoms with a periodic slab of  $3 \times 3$  supercell. To model the doped system various beryllium (Be) and nitrogen (N) atoms were substituted into the stanene slab of  $3 \times 3$  supercell, and systematic study on the effects of substituting Be, N and Be-N into stanene on structural and electronic properties were determined and analyzed in detail. A convergence test for interlayer gap has been conducted in order to neglect interlayer interactions, converged value of about 25 Å has been attained. Therefore, we used vacuum space of 25 Å in the z direction to neglect any interaction between the periodic layers (Mohebpour *et al.*, 2025). In structural properties calculations all atoms were allowed to relaxed for both pure and doped systems.

## 3.0 Results and Discussion

### 3.1 Convergence test for e-cut and k-points of pure stanine

A fundamental prerequisite for first-principles calculations within the context of DFT is the execution of convergence test calculation prior to structural, electrical, and optical properties calculation (Itas *et al.*, 2024; Yusuf *et al.*, 2024). Figure 1 results show the outcomes of convergence tests with regard to the plane wave kinetics energy cut-off and k-points mesh, respectively. The convergence test in Figure 1(a) shows that the total energy fluctuates greatly with regard to the kinetic energy cut-off from 10 Ry to 30 Ry and is nearly constant at 40 Ry. Therefore, for all of our computations, we used 50 Ry as the kinetic energy cut-off value. The variations of the total energy with k-points are presented in Figure 1(b). Nevertheless, the total energy changes substantially with the number of k-points signifying a well-converged value at exact points. However, the total energy decreases from  $3 \times 3 \times 1$  to  $8 \times 8 \times 1$  k-point grids and remain almost steady at  $8 \times 8 \times 1$  k-points. Therefore,  $12 \times 12 \times 1$  k-point is used for all our calculations.

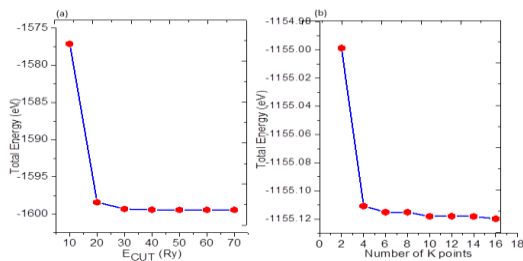


**Figure 1:** (a) Convergence of kinetic energy cut-off with respect to total energy (b) Convergence of k-points grids with respect to the total energy.

### 3.2 Structural and electronic properties of pure stanene

Primitive unit cell of stanene contained two atoms of tin (Sn) arranged in hexagonal structure (Shuaibu *et al.*, 2021; Taura *et al.*, 2021). As a results of weak  $\pi$ - $\pi$  bonding between the Sn-Sn atom, Sn has buckling geometry. The structure of  $3 \times 3$  supercell of stanene containing 18 atoms of tin as displayed in Figure 2(a). The computed lattice parameter of  $3 \times 3$  supercell of stanene with inclusion of SOC and vdW corrections were found to be  $a=b=4.66$  Å and this value is consistent with experimental value of 4.67 Å (Ochapski & De Jong, 2022). The calculated bond length and bond angle of 2.920 Å and 111.6° with the most recent vdW functional (vdW-DFC09x) matched very well with experimental results of 2.94 Å (Deng *et al.*, 2018). The buckling height of 0.87 Å is in good agreement with experimental measurement of 0.85 Å (Ochapski & De Jong, 2022). It was reported that the most stable Sn is the buckling form due to the weak  $\pi$ - $\pi$  interaction, which is difference from planar geometry of graphene. Also, by setting Fermi level to zero, the calculated electronic band structure of pristine stanene with and without SOC are displayed in Figure 2 (b) and 2 (c).

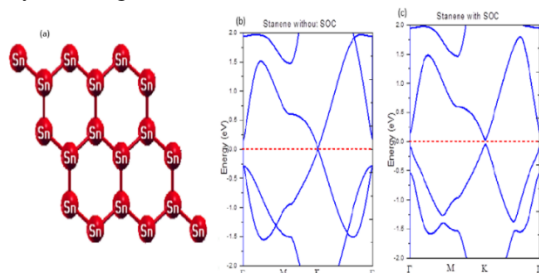


**Figure 2:** (a) Relaxed structure (b) Band structure without SOC (c) Band structure with SOC of a  $3 \times 3$  supercell of a pristine Sn sheet.

Figure 2 (b) revealed that the calculated band structure of stanene without taken into account the effect of SOC is a gapless material, and the Dirac cone is located at K-point and this matched very well with previous results (Abbasi, 2019; Abbasi & Sardroodi, 2018). Figure 2 (c) shows that addition of SOC and vdW-DFC09x open a reasonable band gap of about 0.1 eV. This open up the possibility of utilizing stanene for highly efficient integrated circuits

(ICs) (Liu *et al.*, 2011). Interestingly, stanene behave like quantum spin hall insulator (QSHI) by adding SOC (Xu *et al.*, 2013). Furthermore, metallic nature of pure stanene is the limitation that prevent utilizing it for future optoelectronic devices such as solar cell, photodetector etc. Hence, doping stanene with non-metal elements such as nitrogen (N) and beryllium (Be) can make it a promising candidate for numerous applications like solar cell. Hence, significant improvements can be achieved by doping pure stanene with different elements like N and Be atoms by using substitution method. Generally, doping using substitutional method is a well-known approach for tuning the electronic properties of materials. The electronic properties of stanene and graphene are similar because is the fourth member of carbon family, therefore, band gap opening is possible by simple mono- (Be, N) doping and co-doping (Be-N). The results of Beryllium (Be) doped stanene indicated its potential as a promising candidate for optoelectronic applications. Previous study demonstrated that substituting Be in graphene nanosheet open its band gap to about 0.298 eV, signifying Be doped graphene as a semiconductor material (López-Urías *et al.*, 2015). Here, we have taken Be doping into account in the amounts of 5.67 %, 11.11 % and 16.67 %. In order to achieved 5.6 %, 11.11 % and 16.67 % doping concentration one, two and three atoms of Be were substituted into the tin vacancy of  $3 \times 3$  supercell of Sn sheet containing 18 atoms. Here, we have taken Be doping into account in the amounts of 5.6 %, one Be atom was substituted into 18 atoms of stanene supercell. Moreover, because of the difference in atomic radius, the structure warps more. For full first principles calculation, we have also relaxed Be doped stanene in order to obtained the optimized parameters, it was found from the results that Be doped stanene has buckling structure similar to pure stanene. The buckling height of Be doped stanene was found to be 0.89 Å and this value is higher than that of pure stanene. The electronic structure in Figure 3 (b) demonstrates that the Fermi level is shifted towards the valence band edge in comparison to pure stanene due to deficiency of electron in Be in relation to Sn, indicating that stanene doped beryllium is a p-type material. In this work, the Dirac cone was found to be shifted by 0.28 eV from the Fermi level. This helps to explain the change in electronic properties caused by Be-doping. Therefore, Be doped stanene exhibits a band gap above the Fermi level of 0.29, 0.56 and 1.1 eV for 5.6 %, 11.1 % and 16.7 % concentrations, indicating that Be doped stanene could behave as a degenerate semiconductor. Band structure analysis of Be doped Sn shows that the band gap value increases as the concentration of the dopant increases.

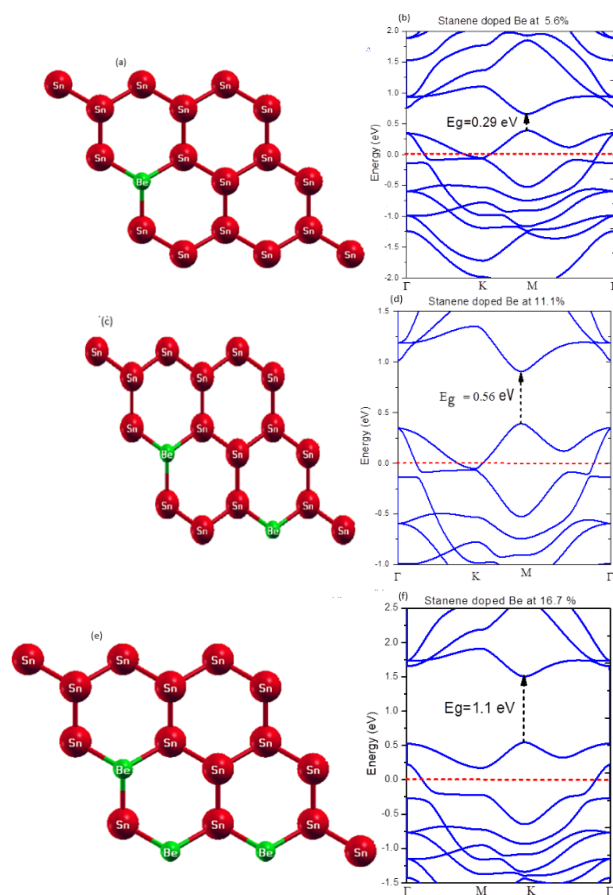


**Figure 3:** Relaxed structure of Be doped stanene at different impurity concentration (a) 5.6 % (c) 11.1 % (e) 16.7 % and band structure of Be doped stanene at different impurity concentration (b) 5.6 % (d) 11.1 % (f) 16.7 %

Experimental and theoretical studies have shown that N doped graphene is a promising candidate for optoelectronic applications such as catalysis and solar cell applications (Olaniyan *et al.*, 2018; Wang *et al.*, 2012). Therefore, we expect that N doped stanene might demonstrate similar band structure as that of N doped graphene. Thus, we have calculated the electronic properties of N doped Sn by substituted one, two and three atoms of N in the stanene supercell containing 18 atoms which also corresponds to 5.6 %, 11.1 % and 16.7 % concentrations. Figure 4 (a), (c) and (e) show the relaxed structure of N doped stanene and the buckling parameter were found to be 0.90 Å and this value is almost the same as that of Be doped stanene. In addition, the calculated Sn-N bond length was also found to be 2.26 Å and this value is significantly lower than that of Sn-Sn (2.920 Å). The electronic band structure in Figure 4 (b), (d) and (f) show that the Fermi levels were shifted towards conduction band edge when compared to pure stanene, demonstrating that stanene doped with nitrogen is an n-type material and providing insight into the change in electronic properties brought on by N-doping. The n-type nature of N doped stanene is in good agreement

with previous first principles calculation (Garg *et al.*, 2017). The band-gap below the Fermi level were 0.30, 0.45 and 0.96 eV for 5.6 %, 11.1 % and 16.7 % doping concentrations. Furthermore, in our studies we observed that the Dirac cone exists for both Be- and N-doped Stanene while in the previous study the Dirac cone vanished in the case of N doped stanene (Garg *et al.*, 2017). The discrepancy between our results and that of Garg *et al.* (Garg *et al.*, 2017) could be due to low concentration level or lack of inclusion of van der Waals correction in their calculation. This suggests that N doped stanene is an n-type material. Additionally, the structure shows more distortion around the N-centre and this can be understood from the Sn-N bond distance (2.26 Å) in comparison to Sn-Sn bond. Thus, our studies suggested that N doped stanene could be a promising candidate for optoelectronic application similar to N doped graphene.

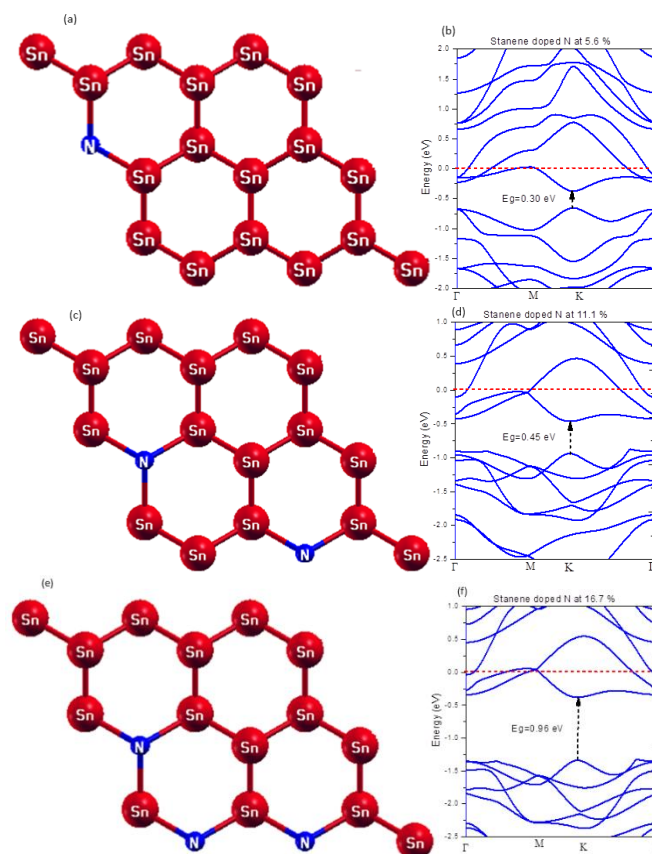


**Figure 4:** Relaxed structure of N doped stanene at different impurity concentration (a) 5.6 % (c) 11.1 % (e) 16.7 % and band structure of N doped stanene at different impurity concentration (b) 5.6 % (d) 11.1 % (f) 16.7 %

Finally, we have also considered Be-N co-doped stanene to compare the results to that of mono-doping and see if there is improvement for band gap opening in stanene.



Furthermore, Olaniyan *et al.* (2018) have investigated the stability, electronic and optical properties of beryllium and nitrogen co-doped graphene phases using Projected Augmented Wave (PAW) with the Generalized Gradient Approximation as proposed by Perdew Burke Ernzerhof (PBE). In their studies they found that Be-N co-doped graphene is a promising candidate for various applications such as optoelectronic and nano-electronic devices (Olaniyan *et al.*, 2018). Additionally, Be-N co-doping induces electron (e) and hole (h) concurrently. Therefore, there is possibility of wider band gap opening in stanene. For this, we have performed band structure calculations of Be-N co-doped Sn using nearest-neighbours configuration. In the case of Be-N co-doped Sn two atoms of  $3 \times 3$  Sn supercell was substituted by a pair of Be and N atoms which corresponding to 11.1 % of B-N doping. In our arrangement, Be and N atoms were co doped in a way such that the distance between them is the lowest to for the formation of covalent bond. The electronic band structure of Be-N co-doped Sn is depicted in Figure 4 (a) and the results shown that the Fermi level is shifted towards the valence band edge when compared to that of pure stanene, which indicates that stanene co-doped Be-N is also a p-type material and this helps to explain the change in electronic properties caused by Be-N co-doping. Moreover, Dirac cone in the band structure plots of Be-N co-doped Sn vanished at the Fermi level whereas in the case of Be- and N-doped Sn there is existence of Dirac cone at the Fermi level. However, a band value of 1.24 eV formed above the Fermi level, indicating that Be-N co-doped Sn is degenerate semiconductor material. Accordingly, our findings suggested that Be-N co-doped Sn is a promising material for optoelectronic and other application like Be-N co-doped graphene.

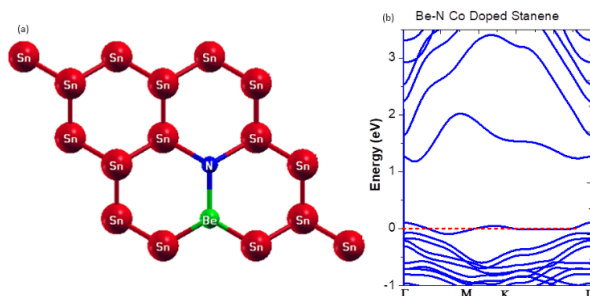


**Figure 5:** (a) Relaxed structure of Be-N co-doping stanene (b) band structure of Be-N co-doping stanene

## 5.0 Conclusion

In this paper, first-principles approached were used to investigate the structural and band structure of the effects of Be and N mono-doped and co-doped stanene to fully exploit the possibility of using stanene as semiconductor material for optoelectronic application. Kinetic energy cut-off convergence test revealed that total energy fluctuates greatly with regard to the kinetic energy cut-off from 10 Ry

to 30 Ry and is nearly constant at 40 Ry. The results of variations of total energy with k-points shows that total energy decreases substantially from  $3 \times 3 \times 1$  to  $8 \times 8 \times 1$  k-point grids and remain almost steady at  $8 \times 8 \times 1$  k-points. The computed lattice parameter, bond length and bond angles with vdW corrections (vdW-DFC09x) were found to be consistent with experimental value for both Be and N mono-doped and co-doped stanene. The calculated band structure of Be and N mono-doped and co-doped stanene show that addition of impurity opens up a band gaps below and above the Fermi level, indicating a transition from metallic nature to semiconductor. Additionally, Be-N co-doped stanene sheet opens up a wider band gap of 1.24 eV in comparison with the mono Be-and N-doped systems. Our findings suggested that Be-N co-doped stanene is a promising material for optoelectronic, solar and other application like Be-N co-doped.

## Declarations

### Ethics approval and consent to participate

Not Applicable.

### Consent for publication

All authors have read and consented to the submission of the manuscript.

### Availability of data and material

Not Applicable.

### Competing interests

All authors declare no competing interests.

## References

- Abbasi, A. (2019). DFT study of the effects of AlP pair doping on the structural and electronic properties of stanene nanosheets. *Physica E: Low-dimensional Systems and Nanostructures*, 108, 34-43.
- Abbasi, A., & Sardroodi, J. J. (2018). Electronic structure tuning of stanene monolayers from DFT calculations: Effects of substitutional elemental doping. *Applied Surface Science*, 456, 290-301.
- Baig, N. (2023). Two-dimensional nanomaterials: A critical review of recent progress, properties, applications, and future directions. *Composites Part A: Applied Science and Manufacturing*, 165, 107362.
- Chaves, A., Azadani, J. G., Alsalman, H., Da Costa, D., Frisenda, R., Chaves, A. Zhou, J. (2020). Bandgap engineering of two-dimensional semiconductor materials. *npj 2D Materials and Applications*, 4(1), 29.
- Chen, Z., Li, R., Bai, Y., Mao, N., Zeer, M., Go, D.,...Niu, C. (2024). Topology-engineered orbital Hall effect in two-dimensional ferromagnets. *Nano Letters*.

- Deng, J., Xia, B., Ma, X., Chen, H., Shan, H., Zhai, X. Duan, W. (2018). Epitaxial growth of ultraflat stanene with topological band inversion. *Nature materials*, 17(12), 1081-1086.
- Garcia, J. C., De Lima, D. B., Assali, L. V., & Justo, J. F. (2011). Group IV graphene-and graphane-like nanosheets. *The Journal of Physical Chemistry C*, 115(27), 13242-13246.
- Garg, P., Choudhuri, I., Mahata, A., & Pathak, B. (2017). Band gap opening in stanene induced by patterned B–N doping. *Physical Chemistry Chemical Physics*, 19(5), 3660-3669.
- Geng, D., & Yang, H. Y. (2018). Recent advances in growth of novel 2D materials: beyond graphene and transition metal dichalcogenides. *Advanced Materials*, 30(45), 1800865.
- Gidado, A. S., Abubakar, L., Taura, L. S., Lawal, A., & Isah, A. (2024). Structural, Electronic, and Optical Properties of Stanene and Stanene-Doped Non-metals for Optoelectronics Applications: A first-principle Study. *Physics Access*, 4(1), 8-20.
- Itas, Y. S., Razali, R., Tata, S., Kolo, M., Lawal, A., Alrub, S. A., Khandaker, M. U. (2024). DFT studies on the effects of C vacancy on the CO<sub>2</sub> capture mechanism of silicon carbide nanotubes photocatalyst (Si<sub>12</sub>C<sub>12</sub>-X; X= 1; 2). *Silicon*, 16(1), 241-251.
- Itas, Y. S., Suleiman, A. B., Ndikilar, C. E., Lawal, A., Razali, R., Ullah, M. H. Khandaker, M. U. (2023). DFT studies of the photocatalytic properties of MoS<sub>2</sub>-doped boron nitride nanotubes for hydrogen production. *ACS omega*, 8(41), 38632-38640.
- Lawal, A., Shaari, A., Taura, L., Radzwan, A., Idris, M., & Madugu, M. (2021). G0W0 plus BSE calculations of quasiparticle band structure and optical properties of nitrogen-doped antimony trisulfide for near infrared optoelectronic and solar cells application. *Materials Science in Semiconductor Processing*, 124, 105592.
- Liu, C.-C., Jiang, H., & Yao, Y. (2011). Low-energy effective Hamiltonian involving spin-orbit coupling in silicene and two-dimensional germanium and tin. *Physical Review B*, 84(19), 195430.
- Liu, Y., Mu, D., & Zhuang, J. (2022). Group IVA of 2D xenes materials (silicene, germanene, stanene, plumbene). In *2D Monoelemental Materials (Xenes) and Related Technologies* (pp. 39-66). CRC Press.
- López-Urías, F., Terrones, M., & Terrones, H. (2015). Beryllium doping graphene, graphene-nanoribbons, C60-fullerene, and carbon nanotubes. *Carbon*, 84, 317-326.
- Mohebpour, M. A., Seriani, N., & Tagani, M. B. (2025). Electronic and optical properties of InSe/CuI van der Waals heterostructure with type-II band alignment: Effects of vertical strain and electric field. *Materials Today Communications*, 42, 111059.
- Mubashir, M., Ali, M., Bibi, Z., Afzal, U., Albaqami, M. D., Mohammad, S., & Muzamil, M. (2024). Computational evaluation of novel XCuH<sub>3</sub> (X= Li, Na and K) perovskite-type hydrides for hydrogen storage applications using LDA and GGA approach. *Journal of Molecular Graphics and Modelling*, 131, 108808.
- Nagarajan, V., & Chandiramouli, R. (2017). Investigation of electronic properties and spin-orbit coupling effects on passivated stanene nanosheet: A first-principles study. *Superlattices and Microstructures*, 107, 118-126.
- Nandee, R., Chowdhury, M. A., Shahid, A., Hossain, N., & Rana, M. (2022). Band gap formation of 2D material in graphene: Future prospect and challenges. *Results in Engineering*, 15, 100474.
- Ochapski, M. W., & De Jong, M. P. (2022). Progress in epitaxial growth of stanene. *Open Physics*, 20(1), 208-223.
- Olaniyan, O., Maphasha, R., Madito, M., Khaleed, A., Igumbor, E., & Manyala, N. (2018). A systematic study of the stability, electronic and optical properties of beryllium and nitrogen co-doped graphene. *Carbon*, 129, 207-227.
- Qi, C., Jiang, F., & Yang, S. (2021). Advanced honeycomb designs for improving mechanical properties: A review. *Composites Part B: Engineering*, 227, 109393.
- Shuaibu, A., Tanko, Y. A., Abdurrahman, Z., Lawal, A., & Nasir, M. M. (2021). Effect of Beryllium and Magnesium Doped Stanene Single Layer on Structural and Electronic Properties Using Density Functional Theory as Implemented in Quantum ESPRESSO. *Physics Access*, 1.
- Tang, X., Fan, T., Wang, C., & Zhang, H. (2021). Halogen functionalization in the 2D material flatland: strategies, properties, and applications. *Small*, 17(24), 2005640.

- Taura, L., Abdulmalik, I., Gidado, A., & Lawal, A. (2021). Structural, Electronic and Optical Properties of Stanene Doped Beryllium: A First Principle Study. *Phys. Sci. Int. J.*, 32-40.
- Wang, H., Maiyalagan, T., & Wang, X. (2012). Review on recent progress in nitrogen-doped graphene: synthesis, characterization, and its potential applications. *ACS catalysis*, 2(5), 781-794.
- Wang, J., Xu, Y., & Zhang, S.-C. (2014). Two-dimensional time-reversal-invariant topological superconductivity in a doped quantum spin-Hall insulator. *Physical Review B*, 90(5), 054503.
- Xu, Y., Tang, P., & Zhang, S.-C. (2015). Large-gap quantum spin Hall states in decorated stanene grown on a substrate. *Physical Review B*, 92(8), 081112.
- Xu, Y., Yan, B., Zhang, H.-J., Wang, J., Xu, G., Tang, P., Zhang, S.-C. (2013). Large-gap quantum spin Hall insulators in tin films. *Physical review letters*, 111(13), 136804.
- Yang, F., Hu, P., Yang, F., Hua, X.-J., Chen, B., Gao, L., & Wang, K.-S. (2024). Photocatalytic applications and modification methods of two-dimensional nanomaterials: a review. *Tungsten*, 6(1), 77-113.
- Yusuf, I. D., Suleiman, A. B., Lawal, A., Ndikilar, C. E., Taura, L., Gidado, A., & Chiromawa, I. M. (2024). Significant improvement in Structural, Electronic, Optical and Thermoelectric properties of PdTe<sub>2</sub> In bulk and Monolayer Phase: A G0W0+ BSE Approach. *Physica B: Condensed Matter*, 416015.
- Zhang, G.-F., Li, Y., & Wu, C. (2014). Honeycomb lattice with multiorbital structure: Topological and quantum anomalous Hall insulators with large gaps. *Physical Review B*, 90(7), 075114.
- Zhao, J., Liu, G., Wei, L., Jiao, G., Chen, Y., Yang, Z., & Zhang, G. (2024). Density functional theory study on the electronic and optical properties of full-hydrogenated stanene. *Modern Physics Letters B*, 38(19), 2450159.